

Covariant nonlocal chiral quark model and pion-photon transition distribution amplitudes

Piotr Kotko* and Michal Praszalowicz†

M. Smoluchowski Institute of Physics, Jagiellonian University, Reymonta 4, 30-059 Kraków, Poland

(Received 30 July 2009; published 2 October 2009)

Using a nonlocal chiral quark model with simple pole ansatz for the momentum dependence of the constituent quark mass and nonlocal currents satisfying Ward-Takahashi identities, we calculate pion-to-photon transition distribution amplitudes and relevant form factors. For vector amplitude we recover correct normalization fixed by the axial anomaly. We find that due to the nonlocality in the vector current, the value of the axial form factor at zero momentum transfer is lowered with respect to the vector form factor. Such behavior—consistent with experiment—is not seen in the local models. Where possible we compare our results to the experimental data.

DOI: 10.1103/PhysRevD.80.074002

PACS numbers: 12.39.Ki, 13.40.Gp

I. INTRODUCTION

Transition distribution amplitudes (TDA) were first introduced in Ref. [1] as objects parametrizing the soft part of the amplitudes for hadron-antihadron annihilation $\bar{H}H \rightarrow \gamma^* \gamma$ or backward Compton scattering $\gamma^* H \rightarrow H \gamma$, where the hard scale is provided by high virtuality of one of the photons. In some sense TDA's are hybrids of the ordinary distribution amplitudes (DA) and generalized parton distributions (GPD) (see [2] for a review). However, if one restricts oneself to the mesonic case, they are more similar to GPD's—the difference is that we deal with matrix elements which are nondiagonal not only in momenta but in the physical states as well. Nevertheless, from a kinematical point of view, both are almost identical and therefore we can use similar variables as skewedness, for example. In practice we consider two kinds of TDA's: vector and axial, depending on nature of the bilocal quark-antiquark operator sandwiched between photon and meson states. For experimental issues of transition distribution amplitudes, see Ref. [3].

In order to avoid complexity of bound state physics, we limit ourselves to pions only. Pions are Goldstone bosons of broken SU(2) chiral symmetry and their properties are to a large extent determined by the symmetry (breaking) alone rather than by the complex phenomenon of confinement. After such simplification, we can use the nonlocal semibosonized Nambu-Jona-Lasinio (NJL) model to get an insight into TDA's. On the other hand, since transition distribution amplitudes are related to anomalous diagrams, they can serve as a demanding tester of the nonlocal models. We shall come back to this point later in this paper.

First estimates of TDA's were made in Refs. [4–6]. The first one [4] was based on general QCD symmetries supported by a simple quark model, while the second [6] and the third one [5] made use of the spectral quark model [7] and Pauli-Villars regulated NJL, respectively. The calcu-

lations in the spectral quark model respect all QCD symmetries by definition (i.e., Lorentz invariance, Ward identities, anomalies, etc.). In the Pauli-Villars regulated NJL model, the presence of the finite regulator [5] gives normalization for the vector amplitude which is not consistent with axial anomaly. In [8] we calculated TDA's numerically in the nonlocal chiral quark model, however, since we have used “naive” currents we also broke the normalization condition of the vector TDA.

In the present paper, we extend our calculations from Ref. [8] in a twofold way: we use the full nonlocal vertices and obtain not only numerical but also analytical results for some of the TDA's. As a result, we recover correct normalization of the vector amplitude and give reliable predictions for the axial form factor which is not restricted by anomaly. Our results are in qualitative agreement with experimental data. Since we revised our old calculations using different method, we traced the mistake in the vector amplitude, which however does not change the qualitative results.

The paper is organized as follows. In Sec. II, we review the nonlocal chiral quark model and give the prescription for modified currents. Next, in Sec. III, we recall the definitions of TDA's and relevant sum rules. Section IV contains our results with special emphasis on the role of the new pieces coming from the nonlocal parts of the currents. In Sec. V, we investigate the relevant form factors and finally we summarize our results in Sec. VI. Technical details are given in the Appendixes.

II. NONLOCAL COVARIANT CHIRAL QUARK MODEL

In the following we use the nonlocal semibosonized Namu-Jona-Lasinio model. It is based on the quark-pion interaction in the following form [9]:

$$S_{\text{Int}} = \int \frac{d^4 k d^4 l}{(2\pi)^8} \bar{\psi}(k) \sqrt{M(k)} U^{\gamma_5}(k-l) \sqrt{M(l)} \psi(l), \quad (1)$$

where $M(k)$ is a dynamical quark mass appearing due to

*kotko@th.if.uj.edu.pl

†michal@if.uj.edu.pl

the spontaneous chiral symmetry breaking. Meson field U^{γ_5} is given in terms of the pion field as

$$U^{\gamma_5}(x) = \exp\left\{\frac{i}{F_\pi} \tau^a \pi^a(x) \gamma_5\right\}, \quad (2)$$

where $F_\pi = 93$ MeV is the pion decay constant.

One defines the momentum dependence of the mass as

$$M(k) = MF^2(k) \quad (3)$$

where form factor $F(k)$ should vanish for $k \rightarrow \infty$ and is chosen to satisfy $F(0) = 1$. Expression for $F(k)$ was obtained analytically in Euclidean space from the instanton model of the QCD vacuum and it is highly nontrivial [9]. Therefore here we use the Minkowski form proposed in [10]

$$F(k) = \left(\frac{-\Lambda_n^2}{k^2 - \Lambda_n^2 + i\epsilon}\right)^n, \quad (4)$$

which reproduces reasonably well the instanton result when continued to Euclidean space. However, it can be also used directly in the Minkowski space. Integer parameter n defines a family of models and allows to analyze a dependence of our results on the shape of $F(k)$. It was argued in Ref. [11] that $F(k)$ should vanish exponentially for large momenta in order to be consistent with operator-product expansion method. This is another reason for introducing n parameter, which allows to control high momentum behavior. The method of fixing the value of Λ_n is described below.

It is a well known fact that due to the momentum dependence of the mass the standard vector and axial currents are not conserved and Ward-Takahashi (WT) identities are not satisfied. Although it was argued in Ref. [8] that this violation is not very large and almost does not affect shapes of TDA's, it certainly affects overall normalizations. It is therefore necessary to resolve the problem of normalization if one wants to use TDA's calculated in the nonlocal model for phenomenological estimates.

There are several ways of constructing conserved currents in the presence of nonlocal interactions; see Refs. [12–16]. However, it should be recalled at this point that none of them is unique, because current conservation fixes only the longitudinal part of a given vertex while the transverse one has to be modeled. In this paper we use the simplest “minimal” vertices satisfying WT identities. For vector current $j^\mu = \bar{\psi} \gamma^\mu \psi$ we replace γ^μ by the following nonlocal vertex

$$\Gamma^\mu(k, p) = \gamma^\mu + g^\mu(k, p), \quad (5)$$

where the nonlocal addition reads

$$g^\mu(k, p) = -\frac{k^\mu + p^\mu}{k^2 - p^2} (M(k) - M(p)). \quad (6)$$

This form of nonlocality does not introduce singularities as required by general properties of vector vertices [13].

Axial current $j_5^\mu = \bar{\psi} \gamma^\mu \gamma_5 \psi$ is made conserved by replacing $\gamma^\mu \gamma_5$ by

$$\Gamma_5^\mu(k, p) = \gamma^\mu \gamma_5 + g_5^\mu(k, p), \quad (7)$$

with

$$g_5^\mu(k, p) = \frac{p^\mu - k^\mu}{(p - k)^2} (M(k) + M(p)) \gamma_5. \quad (8)$$

In contrary to the vector vertex, the axial one contains physical singularity corresponding to the pion.

For a model given by n we fix Λ_n using the Birse-Bowler [15] formula for the pion decay constant F_π :

$$F_\pi^2 = \frac{N_c}{4\pi^2} \times \int_0^\infty dk_E^2 k_E^2 \frac{M^2(k_E) - k_E^2 M(k_E) M'(k_E) + k_E^4 M'(k_E)^2}{(k_E^2 + M^2(k_E))^2} \quad (9)$$

with $F_\pi = 93$ MeV. The prime denotes differentiation with respect to k_E^2 . Using (4) this expression can be calculated analytically; see the Appendix of [17]. In Table I we present Λ_n for given values of constituent quark mass M and power n . Let us recall at this point that there exists another expressions for F_π , namely, the Pagels-Stokar formula [12]. As shown explicitly in, e.g., [18], it accommodates a nonlocal pion-quark interaction, however it corresponds to the naive axial current j_5^μ which, as mentioned above, does not exhibit partial conservation of axial current. On the contrary, the Birse-Bowler formula [15] takes into account the nonlocal axial current (more precisely its derivative, which is determined unambiguously); see Ref. [18] for discussion.

It is important to note that Λ_n *does not correspond* to the QCD scale characteristic for the present model. Indeed function $F(k)$ does not change much for different (n, Λ_n) except for the high momentum part. Therefore, as pointed out in [8, 19], the precise definition of the scale can be done only within QCD, while within an effective model one can only estimate the order of magnitude. For the instanton

TABLE I. Numerical values of the model parameters obtained using Birse-Bowler formula (9) for the pion decay constant F_π .

$M = 225$ MeV	
$n = 1$	$\Lambda = 1641$ MeV
$n = 5$	$\Lambda = 3823$ MeV
$M = 350$ MeV	
$n = 1$	$\Lambda = 836$ MeV
$n = 5$	$\Lambda = 1970$ MeV
$M = 400$ MeV	
$n = 1$	$\Lambda = 721$ MeV
$n = 5$	$\Lambda = 1704$ MeV

model the characteristic scale is about 600 MeV [9]. A somewhat more detailed discussion of this issue can be found in Ref. [19].

The nonlocal model with momentum dependent quark mass given by (4) was applied in the past to several low energy quantities (pion DA [10], two pion generalized DA [20], quark and gluon condensates [19]), using however naive vector and axial currents. Later in Ref. [18], pion DA with conserved axial current was estimated using partially conserved axial current. Recently a set of photon DA's up to twist-4 was obtained using currents satisfying WT identities [17].

Similar models with however different form of $F(k)$ in (3) were also considered in the literature. In Ref. [15] exponential form of $F(k)$ was used. In Refs. [21–26] various distribution amplitudes and correlators have been studied in nonlocal models similar to ours. Pion and kaon DA were also calculated in [27].

III. KINEMATICS AND DEFINITIONS

Relevant kinematics is very close to the one used in GPD formalism. We consider pion with momentum P_1 and real photon carrying momentum P_2 . We shall work in the chiral limit, therefore both $P_1^2 = 0$ and $P_2^2 = 0$. We define momentum transfer $q^\mu = P_2^\mu - P_1^\mu$ and momentum transfer squared $t = q^2$. Two lightlike directions are defined by null vectors $n = (1, 0, 0, -1)$ and $\tilde{n} = (1, 0, 0, 1)$. Decomposition of any vector v^μ in this basis reads

$$v^\mu = v^+ \frac{\tilde{n}^\mu}{2} + v^- \frac{n^\mu}{2} + v_T^\mu, \quad (10)$$

while the scalar product

$$u \cdot v = \frac{1}{2}u^+ v^- + \frac{1}{2}u^- v^+ - \vec{u}_T \cdot \vec{v}_T, \quad (11)$$

where arrows denote Euclidean two-vectors. Introducing average momentum $p = \frac{1}{2}(P_1 + P_2)$ we can define so-called skewedness variable

$$\xi = -\frac{q^+}{2p^+}. \quad (12)$$

For massless pions $-1 < \xi < 1$. Switching to the frame where the average momentum does not have a transverse part, i.e.,

$$p^\mu = p^+ \frac{\tilde{n}^\mu}{2} + \frac{p^2}{p^+} \frac{n^\mu}{2}, \quad (13)$$

we can write the following parametrizations of the pion and photon momenta

$$P_1^\mu = (1 + \xi)p^+ \frac{\tilde{n}^\mu}{2} + (1 - \xi) \frac{p^2}{p^+} \frac{n^\mu}{2} - \frac{1}{2}q_T^\mu \quad (14)$$

$$P_2^\mu = (1 - \xi)p^+ \frac{\tilde{n}^\mu}{2} + (1 + \xi) \frac{p^2}{p^+} \frac{n^\mu}{2} + \frac{1}{2}q_T^\mu. \quad (15)$$

Notice that $p^2 = -t/4$. We denote the photon polarization vector by ε . It satisfies condition $\varepsilon \cdot P_2 = 0$.

We can now define TDA's. Vector transition distribution amplitude (VTDA) $V(X, \xi, t)$ is defined as

$$\begin{aligned} \int \frac{d\lambda}{2\pi} e^{i\lambda X p^+} \langle \gamma(P_2, \varepsilon) | \bar{d}\left(-\frac{\lambda}{2}n\right) \Gamma^\mu u\left(\frac{\lambda}{2}n\right) | \pi^+(P_1) \rangle \\ = \frac{i^2 e}{2\sqrt{2}F_\pi p^+} \varepsilon^{\mu\nu\alpha\beta} \varepsilon_\nu^* p_\alpha q_\beta V(X, \xi, t). \end{aligned} \quad (16)$$

In the axial channel the axial transition distribution amplitude (ATDA) $A(X, \xi, t)$ is defined as

$$\begin{aligned} \int \frac{d\lambda}{2\pi} e^{i\lambda X p^+} \langle \gamma(P_2, \varepsilon) | \bar{d}\left(-\frac{\lambda}{2}n\right) \Gamma_5^\mu u\left(\frac{\lambda}{2}n\right) | \pi^+(P_1) \rangle \\ = \frac{ie}{2\sqrt{2}F_\pi p^+} P_2^\mu q \cdot \varepsilon^* A(X, \xi, t) + q^\mu q \cdot \varepsilon^* \\ \times \frac{ie2\sqrt{2}F_\pi \text{sign}(\xi)}{t} \phi_\pi\left(\frac{X + \xi}{2\xi}\right) + \dots \end{aligned} \quad (17)$$

Notice that we have explicitly written down the contribution containing massless pole $1/t$ coming from the fact that the pion can couple directly to the axial current. This part is connected with the pion DA $\phi_\pi(u)$. Dots stand for the remaining parts which vanish when contracted with n^μ [4].

There exist the following sum rules for TDA's:

$$\begin{aligned} \int_{-1}^1 dX \begin{cases} V(X, \xi, t) \\ A(X, \xi, t) \end{cases} &= \frac{2\sqrt{2}F_\pi}{m_\pi} \begin{cases} F_V(t) \\ F_A(t) \end{cases} \\ &= 2\sqrt{2}F_\pi \begin{cases} F_V^X(t) \\ F_A^X(t) \end{cases}, \end{aligned} \quad (18)$$

where $F_V(t)$ and $F_A(t)$ are vector and axial form factors, respectively. Quantity $F_{V,A}^X(t) = F_{V,A}(t)/m_\pi$ is introduced because we work in the chiral limit (m_π is the mass of the pion). Moreover the transition form factor for the process $\pi^0 \rightarrow \gamma^* \gamma$ is related to the vector form factor by the formula

$$F_{\pi\gamma}(t) = \sqrt{2}F_V^X(t). \quad (19)$$

The value of $F_{\pi\gamma}$ for $t = 0$ is fixed by the axial anomaly and equals

$$F_{\pi\gamma}(0) = \frac{1}{4\pi^2 F_\pi} \approx 0.272 \text{ GeV}^{-1}. \quad (20)$$

There is no such constraint for the axial form factor. See Sec. V for the discussion.

IV. TDA'S IN THE COVARIANT NONLOCAL MODEL

In this section we outline some points of the calculations within the model introduced in the previous section and show our results. More details are given in Appendixes A and B.

A. Vector TDA

In the vector channel direct calculation of the matrix elements gives

$$\begin{aligned} & \int \frac{d\lambda}{2\pi} e^{i\lambda X p^+} \left\langle \gamma(P_2, \varepsilon) \left| \bar{d}\left(-\frac{\lambda}{2}n\right) \Gamma^\mu u\left(\frac{\lambda}{2}n\right) \right| \pi^+(P_1) \right\rangle \\ &= -\frac{\sqrt{2}eMN_c}{F_\pi} (Q_d \mathcal{M}_V^{\mu\nu}(X, \xi, t) \\ & \quad + Q_u \mathcal{M}_V^{\mu\nu}(-X, \xi, t)) \varepsilon_\nu^*, \end{aligned} \quad (21)$$

where N_c is the number of colors, Q_u, Q_d are charges of the pertinent quarks and

$$\begin{aligned} \mathcal{M}_V^{\mu\nu} &= \int \frac{d^4k}{(2\pi)^4} \delta(k^+ - (X-1)p^+) \text{Tr}\{S(k+P_2) \\ & \quad \times \Gamma^\mu(k+P_2, k+P_1) S(k+P_1) \\ & \quad \times \Gamma_5(k+P_1, k) S(k) \Gamma^\nu(k+P_1, k)\} \end{aligned}$$

with

$$S(p) = \frac{1}{\not{p} - M(p)}. \quad (22)$$

In the formula above quark-pion coupling reads

$$\Gamma_5(k, p) = F(k) \gamma_5 F(p). \quad (23)$$

Notice that we have used the nonlocal vertex (5) also in the bilocal currents. This is necessary if one wants to maintain WT identities.

Amplitude $\mathcal{M}_V^{\mu\nu}$, due to the natural splitting of the vector vertices to local and nonlocal parts, can be divided into four pieces

$$\mathcal{M}_V^{\mu\nu} = \mathcal{M}_V^{\mu\nu(0)} + \mathcal{M}_V^{\mu\nu(1)} + \mathcal{M}_V^{\mu\nu(2)} + \mathcal{M}_V^{\mu\nu(3)}. \quad (24)$$

To list them we introduce shorthand notation

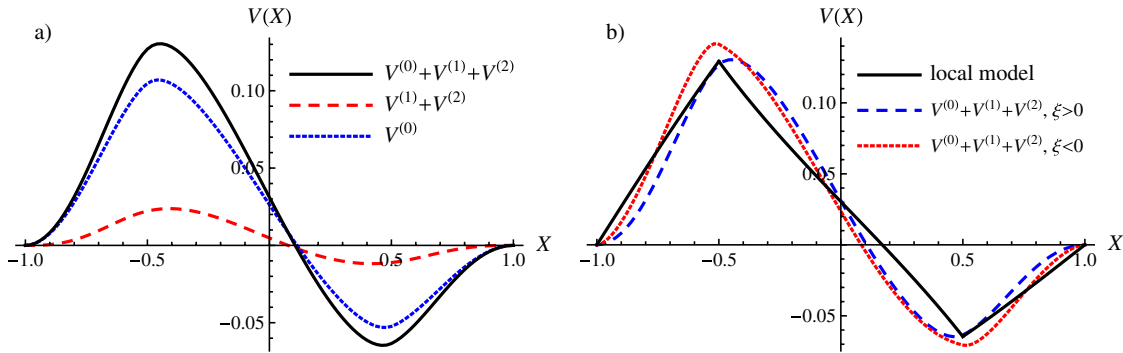


FIG. 1 (color online). Vector TDA for $M = 350$ MeV, $t = -0.1$ GeV², and $n = 1$. (a) Solid line representing full VTDA for $\xi = 0.5$ is the sum of the part coming from the local part of the vector vertex (dotted line) and the nonlocal one (dashed line); (b) comparison of the results of this paper for $\xi = 0.5$ (dashed line), $\xi = -0.5$ (dotted line), and the local version of the model $M(k) = M$ for $\xi = \pm 0.5$.

$$\hat{d}k = \frac{d^4k}{(2\pi)^4} \delta(k^+ - (X-1)p^+). \quad (25)$$

Then

$$\begin{aligned} \mathcal{M}_V^{\mu\nu(0)} &= \int \hat{d}k \text{Tr}\{S(k+P_2) \gamma^\mu S(k+P_1) \\ & \quad \times \Gamma_5(k+P_1, k) S(k) \gamma^\nu\} \end{aligned} \quad (26)$$

corresponds to the quantities calculated in [8]. The new pieces are

$$\begin{aligned} \mathcal{M}_V^{\mu\nu(1)} &= \int \hat{d}k \text{Tr}\{S(k+P_2) \gamma^\mu S(k+P_1) \\ & \quad \times \Gamma_5(k+P_1, k) S(k) g^\nu(k+P_1, k)\}, \end{aligned} \quad (27)$$

$$\begin{aligned} \mathcal{M}_V^{\mu\nu(2)} &= \int \hat{d}k \text{Tr}\{S(k+P_2) g^\mu(k+P_2, k+P_1) \\ & \quad \times S(k+P_1) \Gamma_5(k+P_1, k) S(k) \gamma^\nu\}. \end{aligned} \quad (28)$$

The remaining part of $\mathcal{M}_V^{\mu\nu}$ is zero, simply due to vanishing of the Dirac trace, $\mathcal{M}_V^{\mu\nu(3)} = 0$.

The above decomposition, after projecting on the proper tensor structures, leads straightforwardly to the expression for VTDA

$$V(X, \xi, t) = V^{(0)}(X, \xi, t) + V^{(1)}(X, \xi, t) + V^{(2)}(X, \xi, t). \quad (29)$$

The $V^{(1)} + V^{(2)}$ part is the addition that is required in order to recover correct normalization. The explicit expressions, together with some details needed to calculate $V^{(0)}$ analytically are given in Appendix A.

Our results are shown in Fig. 1. We also plot separately the local part $V^{(0)}$ and the addition $V^{(1)} + V^{(2)}$ itself. We compare the new result with the local version of our model calculated in [8]. Qualitative behavior with M, ξ, n , and t is the same as in [8] therefore we do not discuss this further. However now the condition coming from axial anomaly

$$\int_{-1}^1 V(X, \xi, t) dX = \frac{1}{2\pi^2} \quad (30)$$

is satisfied automatically for any value of n and Λ (which does not have to be necessarily equal Λ_n).

B. Axial TDA

For the matrix element of the axial operator we have

$$\begin{aligned} & \int \frac{d\lambda}{2\pi} e^{i\lambda X p^+} \langle \gamma(P_2, \varepsilon) | \bar{d} \left(-\frac{\lambda}{2} n \right) \Gamma_5^\mu u \left(\frac{\lambda}{2} n \right) | \pi^+(P_1) \rangle \\ &= -\frac{\sqrt{2} e M N_c}{F_\pi} (Q_d \mathcal{M}_A^{\mu\nu}(X, \xi, t) \\ & \quad - Q_u \mathcal{M}_A^{\mu\nu}(-X, \xi, t)) \varepsilon_\nu^* \end{aligned} \quad (31)$$

where

$$\begin{aligned} \mathcal{M}_A^{\mu\nu} &= \int \frac{d^4 k}{(2\pi)^4} \delta(k^+ - (X-1)p^+) \text{Tr}\{S(k+P_2) \\ & \quad \times \Gamma_5^\mu(k+P_2, k+P_1) S(k+P_1) \\ & \quad \times \Gamma_5^\nu(k+P_1, k) S(k) \Gamma^\nu(k+P_1, k)\}. \end{aligned}$$

This expression looks very similar to (21), however here full axial vertex Γ_5^μ given in (7) appears instead of the vector one.

Exploring this expression we find that it has again four parts, similar to the vector case. However, only two of them

contribute to the ATDA, namely,

$$\begin{aligned} \mathcal{M}_A^{\mu\nu(0)} &= \int \hat{d}k \text{Tr}\{S(k+P_2) \gamma^\mu \gamma_5 S(k+P_1) \\ & \quad \times \Gamma_5(k+P_1, k) S(k) \gamma^\nu\} \end{aligned} \quad (32)$$

and

$$\begin{aligned} \mathcal{M}_A^{\mu\nu(1)} &= \int \hat{d}k \text{Tr}\{S(k+P_2) \gamma^\mu \gamma_5 S(k+P_1) \\ & \quad \times \Gamma_5(k+P_1, k) S(k) g^\nu(k+P_1, k)\}. \end{aligned} \quad (33)$$

The remaining terms are connected with pion DA (or they are gauge artifacts). This can be seen by noting that

$$g_5^\mu(k+P_2, k+P_1) = \frac{q^\mu}{t} (M(k+P_2) + M(k+P_1)) \gamma_5 \quad (34)$$

and comparing with definition (17). Therefore we have

$$A(X, \xi, t) = A^{(0)}(X, \xi, t) + A^{(1)}(X, \xi, t), \quad (35)$$

where again $A^{(0)}$ is the old part already calculated in [8]. All further details concerning calculations are relegated to Appendix B.

The results are shown in Fig. 2. It turns out that the integral over dX of the $A^{(1)}(X, \xi, t)$ part is negative, which shifts the value of the axial form factor towards the experimental value. For negative values of ξ the addition

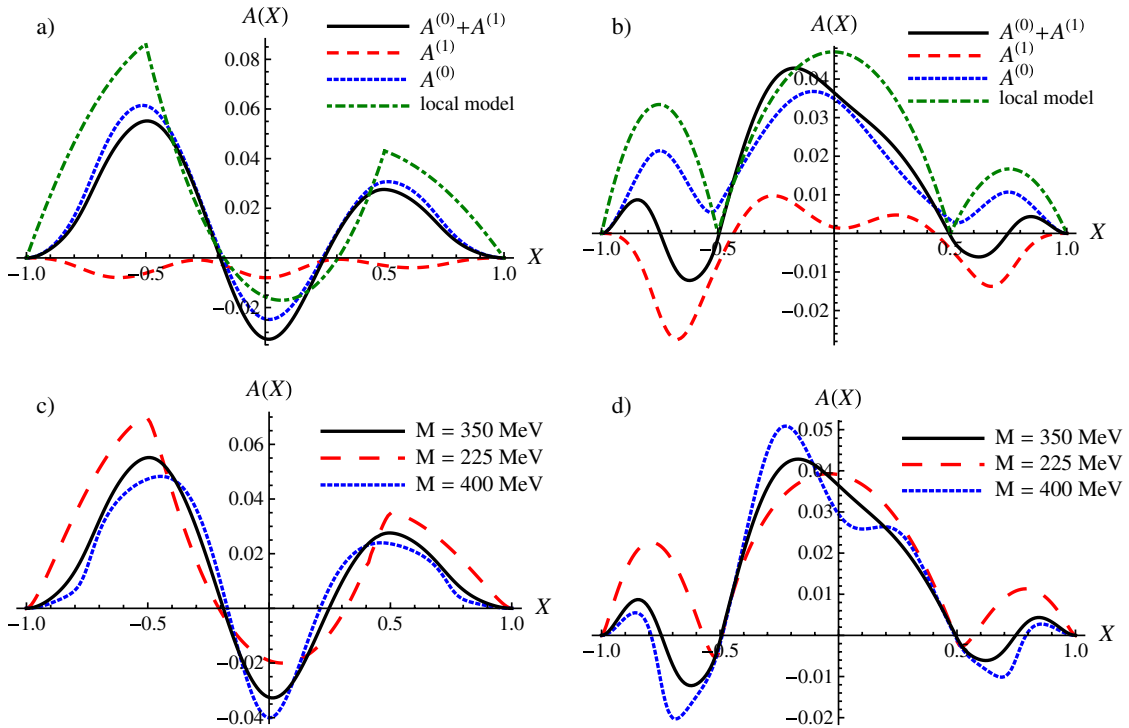


FIG. 2 (color online). Axial TDA for $M = 350$ MeV, $t = -0.1$ GeV², and $n = 1$. (a) Solid line representing full ATDA for $\xi = 0.5$ is the sum of the part coming from the local part of the vector vertex (dotted line) and the nonlocal one (dashed line). The dash-dotted curve is the results for the local model $M(k) = M$. (b) The same for $\xi = -0.5$; (c) results for positive $\xi = 0.5$, $n = 1$, $t = -0.1$ GeV², and different values of M ; (d) the same for negative $\xi = -0.5$.

$A^{(1)}(X, \xi, t)$ has in a sense an unexpected shape, which quite drastically changes the shape of full ATDA for $\xi < 0$. This effect is weaker for lower constituent quark masses as the addition $A^{(1)}$ is proportional to the third power of M/Λ_n . We have checked that for any ξ (both positive and negative)

$$\int_{-1}^1 dXA^{(1)}(X, |\xi|, t) = \int_{-1}^1 dXA^{(1)}(X, -|\xi|, t) = f(t) < 0, \quad (36)$$

where f is some function of t only. Equation (36) is a special case of the polynomiality condition, which is satisfied in our model, both for VTDA and ATDA.

V. FORM FACTORS

As already mentioned in Sec. IV A vector and transition form factors at zero momentum transfer are reproduced correctly, as given by the axial anomaly. Full result for the transition form factor multiplied by momentum transfer is shown in Fig. 3. We make a comparison with CELLO [28], CLEO [29], and some new *BABAR* data [30] for several values of model parameters. Since our approach is reliable at low momenta transfer we limited ourselves to the region of a few GeV^2 . We do not use the standard dipole parametrization for the transition form factor [29] as a reference, because recent *BABAR* data seem to reveal different behavior (see also [31,32]). We find that model parameters $M = 300 \text{ MeV}$ and $n = 1$ fit the data quite well, while low constituent quark masses lie much below. However, we underline that momentum transfer around a few GeV^2 can be too large to be treated within the considered approach.

In the case of the axial form factor, we find that due to the contribution of $A^{(1)}$ its value at zero momentum transfer $F_A(0)$ is lower than for the vector one. The values of $F_A(0)$ and the relevant ratios $F_A(0)/F_V(0)$ for several model parameters are presented in Table II. We notice that when n is increasing, the value of $F_A(0)$ is decreasing very slowly. Therefore we conclude that $F_A(0)$ is quite robust as far as model parameters are concerned. Experimental value given by PDG is

TABLE II. Numerical values for axial form factor at zero momentum transfer $F_A(0)$ for different model parameters.

$M[\text{MeV}]$	n	$F_A(0)$	$F_A(0)/F_V(0)$
225	1	0.0217	0.80
350	1	0.0168	0.62
350	5	0.0163	0.60
400	1	0.0161	0.60
400	5	0.0152	0.56

$$F_A^{\text{exp}}(0) = 0.0115 \pm 0.0005 \quad (37)$$

and

$$(F_A(0)/F_V(0))_{\text{exp}} = 0.7^{+0.6}_{-0.2}. \quad (38)$$

Although our predictions are much better than the ones obtained in local models [with $F_A(0) = F_V(0)$] [4–6,8], they still do not agree with experimental value. Notice however that prediction for $F_V(0)$ provided by conservation of vector current and axial anomaly

$$F_V(0) \approx 0.027 \quad (39)$$

overshoots the experimental value (PDG)

$$F_V^{\text{exp}}(0) = 0.017 \pm 0.008. \quad (40)$$

We recall also that our calculations were done in the chiral limit. The effects due to the finite pion mass were discussed in [5] within the local NJL model and turn out to be small.

VI. SUMMARY

In the present paper we have used the instanton motivated nonlocal chiral quark model to compute pion-to-photon transition distribution amplitudes in vector and axial channels defined in Eqs. (16) and (17). Our approach follows closely the approach of Ref. [8] with one important modification. In Ref. [8] we have used the momentum dependent constituent quark mass and the nonlocal pion-quark interaction, however, both vector and axial currents were not modified to satisfy Ward-Takahashi identities. We have argued in [8] that such an approach—although inconsistent—gives reasonable shape for the TDA's missing,

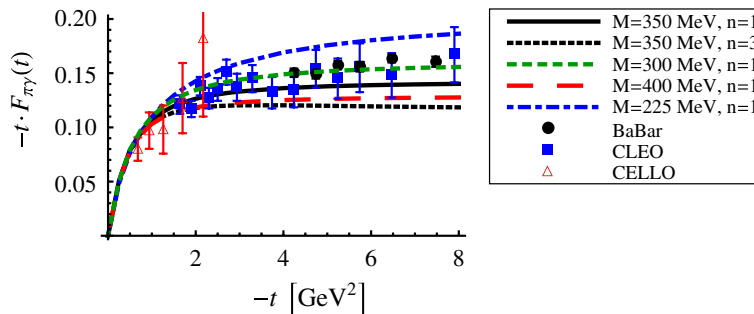


FIG. 3 (color online). Pion-to-photon transition form factor times momentum transfer for several model parameters versus CELLO, CLEO, and *BABAR* data in the 0–8 GeV^2 range.

however, normalization. Indeed, our present findings confirm this conclusion.

In order to satisfy WT identities the naive QCD currents require modifications if the quark mass depends on momentum. Such modifications are not unique because WT identities do not fix the longitudinal part of the current. In the present paper, we have used the simplest possible modifications of the vector and axial currents given by Eqs. (5) and (7).

More importantly, we have used the nonlocal vertex not only for the photon coupling to the quark loop but also for the vector operator defining the TDA. This modification is not obvious for the following reason. Factorization of the physical process into hard and soft parts is done in QCD in terms of the operator product expansion and the relevant operators entering the definition of the soft part are therefore indeed the naive QCD operators. In our language this would correspond to neglecting $\mathcal{M}_V^{\mu\nu,(2)}$ of Eq. (28). We have checked that this would lead to the violation of the normalization condition for VTDA. In the case of ATDA the nonlocal part of the axial current does not contribute, since it enters the piece proportional to the pion DA; see Eq. (17), but not the ATDA itself.

Our findings can be summarized as follows. The normalization of TDA's in the vector channel—which is fixed by the axial anomaly—turns out to be correctly reproduced in our approach. At the same time, normalization of ATDA's is lowered due to the nonlocal term in the vector current. As a result the two normalizations are no longer equal, as observed experimentally. The shapes of the TDA's are similar to the ones obtained in the local model and in the nonlocal model with naive currents. In the case of VTDA's we observe, however, small difference between distributions with positive and negative ξ , which was not the case previously. ATDA's acquire negative contribution from the nonlocal piece which makes the differences between positive and negative ξ 's even more profound than in the previously considered models. We have also investigated dependence of TDA's on the choice of constituent quark mass M and the shape of the cutoff function $F(k)$. Dependence on the power n entering $F(k)$ is rather weak, whereas the dependence on M is effectively important only for ATDA for negative ξ .

We have also calculated the corresponding form factors. The axial form factor is quite robust with respect to the shape of the momentum dependence of the mass. The pion-to-photon transition form factor, which is directly related to the vector form factor, can be compared with experimental data. We compare it with CELLO, CLEO, and recent *BABAR* data in low energy regime in Fig. 3 and conclude that our results reproduce quite well its t dependence.

Let us finish by a remark that we have worked in the chiral limit where $m_\pi = 0$. The effects of adding small current masses are expected to be small, however, only

further study can show whether they will be able to correct small deviations from experimental values of $F_{V,A}(0)$. Finally, the modifications of the nonlocalities that are still possible as far as the longitudinal part of the currents is concerned deserve further investigation.

ACKNOWLEDGMENTS

The authors are grateful to W. Broniowski, E. Ruiz Arriola, and A. Dorokhov for discussions. The paper was partially supported by the Polish-German cooperation agreement between the Polish Academy of Science and DFG.

APPENDIX A: VECTOR TDA

In the beginning, we introduce a shorthand notation in order to make the formulas more compact:

$$M(k) \equiv M_k \quad (\text{A1})$$

and similarly for other k -dependent quantities. We recall that $M_k = MF_k^2$. For the inverse scalar propagators we use

$$D_k = k^2 - M_k^2. \quad (\text{A2})$$

Let us now turn to VTDA. We obtained the following expressions for subsequent pieces giving contribution to $V(X, \xi, t)$

$$V^{(i)}(X, \xi, t) = 16iMN_c p^+ (Q_d I^{(i)}(X, \xi, t) + Q_u I^{(i)}(-X, \xi, t)) \quad (\text{A3})$$

where

$$I^{(0)}(X, \xi, t) = \int \hat{d}k \frac{F_k F_{k+P_1}}{D_{k+P_1} D_{k+P_2} D_k} \times \{F_1(M_{k+P_1} - M_{k+P_2}) + F_2(M_k - M_{k+P_2}) + M_k\}, \quad (\text{A4})$$

$$I^{(1)}(X, \xi, t) = \int \hat{d}k \frac{(-k_T^2 \sin^2 \theta_T) F_k F_{k+P_1} (M_k - M_{k+P_2})}{D_{k+P_1} D_{k+P_2} D_k (k \cdot P_2)}, \quad (\text{A5})$$

$$I^{(2)}(X, \xi, t) = - \int \hat{d}k \frac{(-k_T^2 \sin^2 \theta_T) F_k F_{k+P_1} (M_{k+P_2} - M_{k+P_1})}{D_{k+P_1} D_{k+P_2} D_k (k \cdot q)}. \quad (\text{A6})$$

In the above formulas

$$F_1 = - \frac{\vec{k}_T \cdot \vec{q}_T}{t(1 + \xi)} - \frac{1}{2}(X - 1), \quad (\text{A7})$$

$$F_2 = 2\xi \frac{\vec{k}_T \cdot \vec{q}_T}{t(\xi^2 - 1)} + (X - 1), \quad (\text{A8})$$

and θ_T is an angle between $\vec{\kappa}_T$ and \vec{q}_T in the transverse plane. Integration measure $\hat{d}k$ was introduced in Eq. (25).

As an example, we briefly explain how to calculate $I^{(1)}$. Following Refs. [10], we introduce dimensionless variables $\kappa = k/\Lambda$, $\bar{P}_1 = P_1/\Lambda$, $\bar{P}_2 = P_2/\Lambda$, $r = M/\Lambda$, and use

$$u_{1,2} = (\kappa + \bar{P}_{1,2})^2 - 1 + i\epsilon, \quad (\text{A9})$$

$$u_3 = \kappa^2 - 1 + i\epsilon. \quad (\text{A10})$$

Then using (4) we have

$$I^{(1)}(X, \xi, t) = -\frac{r}{\Lambda^2} \times \int \hat{d}\kappa \frac{\kappa_T^2 \sin^2 \theta_T u_1^{3n} u_2^{2n} u_3^n (u_2^{2n} - u_3^{2n})}{(\kappa \cdot \bar{P}_2) G(u_1) G(u_2) G(u_3)}, \quad (\text{A11})$$

where

$$G(z) = z^{4n+1} + z^{4n} - r^2. \quad (\text{A12})$$

We can obviously write

$$G(z) = \prod_{i=1}^{4n+1} (z - \eta_i), \quad (\text{A13})$$

where η_i 's are the roots of $G(z) = 0$ to be obtained numerically. Their properties were discussed in [10,17]. Then using decomposition into proper fractions we obtain

$$I^{(1)}(X, \xi, t) = -\frac{r}{\Lambda^2} \sum_{i,j,k}^{4n+1} f_i f_j f_k \alpha_{ijk} \tilde{I}_{ijk}^{(1)}(X, \xi, t), \quad (\text{A14})$$

where

$$f_i = \prod_{j \neq i}^{4n+1} \frac{1}{(\eta_i - \eta_j)}, \quad (\text{A15})$$

$$\alpha_{ijk} = \eta_i^{3n} \eta_j^{2n} \eta_k^n (\eta_j^{2n} - \eta_k^{2n}), \quad (\text{A16})$$

and

$$\tilde{I}_{ijk}^{(1)}(X, \xi, t) = \int \hat{d}\kappa \frac{\kappa_T^2 \sin^2 \theta_T}{\kappa \cdot \bar{P}_2 (u_1 - \eta_i)(u_2 - \eta_j)(u_3 - \eta_k)}. \quad (\text{A17})$$

Next we assume that this expression can be continued to the Euclidean space—this is equivalent in Minkowski space to deformation of the $d\kappa^-$ integration contour as described in [10,17]. This choice of the contour assures that the results are real and analytical in Λ_n . The remaining parts of integrals $I^{(0)}$, $I^{(2)}$ can be transformed to a sum of the integrals similarly as in the case $I^{(1)}$. It is convenient to start with the $d\kappa^-$ integration using residue theorem. Positions of the poles in the κ^- complex plane depend on the kinematical region and on the sign of ξ , however the

pole connected with $\kappa \cdot \bar{P}_2$ does not give contribution as it should be. Physical support $-1 < X < 1$ splits into three pieces: $-1 < X < -|\xi|$, $-|\xi| < X < |\xi|$, and $|\xi| < X < 1$. Integrals $I^{(i)}(X, \xi, t)$ are nonzero in the last two, while $I^{(i)}(-X, \xi, t)$ in the first two intervals.

In order to write down the results it is useful to introduce the following notation:

$$g_i^{(A)} = (\kappa_T^2 + 1)(1 - \xi) - \vec{\kappa}_T \cdot \vec{q}_T (X + 1) - (X - 1) \times (1 - 3\xi - X(1 + \xi))\bar{p}^2 + (1 - \xi)\eta_i, \quad (\text{A18})$$

$$g_i^{(B)} = (\kappa_T^2 + 1)(1 - \xi) - \vec{\kappa}_T \cdot \vec{q}_T (X - 1) - (X - 1)^2 \times (1 + \xi)\bar{p}^2 + (1 - \xi)\eta_i, \quad (\text{A19})$$

$$h_i^{(A)} = (\kappa_T^2 + 1)\xi + X\vec{\kappa}_T \cdot \vec{q}_T - (X^2 - 1)\xi\bar{p}^2 + \xi\eta_i, \quad (\text{A20})$$

$$h_i^{(B)} = (\kappa_T^2 + 1)\xi + (X - 1)\vec{\kappa}_T \cdot \vec{q}_T - (X - 1)^2 \xi \bar{p}^2 + \xi \eta_i, \quad (\text{A21})$$

$$d_{ij}^{(AB)} = -2\xi(\kappa_T^2 + 1) - 2X\vec{\kappa}_T \cdot \vec{q}_T + 2(X^2 - 1)\xi\bar{p}^2 + (X - \xi)\eta_i - (X + \xi)\eta_j, \quad (\text{A22})$$

$$d_{ij}^{(AC)} = -(1 + \xi)(\kappa_T^2 + 1) - (1 - X)\vec{\kappa}_T \cdot \vec{q}_T + (1 - \xi) \times (X - 1)^2 \bar{p}^2 + (X + \xi)\eta_i - (X - 1)\eta_j, \quad (\text{A23})$$

$$d_{ij}^{(CB)} = (1 - \xi)(\kappa_T^2 + 1) + (1 - X)\vec{\kappa}_T \cdot \vec{q}_T + (1 + \xi) \times (X - 1)^2 \bar{p}^2 + (X - \xi)\eta_i - (X - 1)\eta_j, \quad (\text{A24})$$

$$\beta_{ijk} = -\alpha_{kji}, \quad (\text{A25})$$

where $\bar{p} = p/\Lambda$ is dimensionless average momentum. Then we have

(i) $|\xi| < X < 1$

$$I^{(0)}(X, |\xi|, t) = I^{(0)}(X, -|\xi|, t) = \frac{1}{2} \frac{ir}{\Lambda p^+} (X - 1) \sum_{i,j,k}^{4n+1} f_i f_j f_k \int \frac{d^2 \kappa_T}{(2\pi)^3} \times \frac{\alpha_{ijk} F_2 + \alpha_{kji} F_1 + \eta_i^{3n} \eta_j^{4n} \eta_k^n}{d_{ki}^{(AC)} d_{kj}^{(CB)}} \quad (\text{A26})$$

$$I^{(1)}(X, |\xi|, t) = I^{(1)}(X, -|\xi|, t) = \frac{ir}{\Lambda p^+} (X - 1)^2 \sum_{i,j,k}^{4n+1} \alpha_{ijk} f_i f_j f_k \times \int \frac{d^2 \kappa_T}{(2\pi)^3} \frac{-\kappa_T^2 \sin^2 \theta_T}{g_k^{(B)} d_{ki}^{(AC)} d_{kj}^{(CB)}} \quad (\text{A27})$$

$$\begin{aligned}
I^{(2)}(X, |\xi|, t) &= I^{(2)}(X, -|\xi|, t) \\
&= \frac{1}{2} \frac{ir}{\Lambda p^+} (X-1)^2 \sum_{i,j,k}^{4n+1} \beta_{ijk} f_i f_j f_k \\
&\quad \times \int \frac{d^2 \kappa_T}{(2\pi)^3} \frac{-\kappa_T^2 \sin^2 \theta_T}{h_k^{(B)} d_{ki}^{(AC)} d_{kj}^{(CB)}}. \quad (A28)
\end{aligned}$$

(ii) $-|\xi| < X < |\xi|$

$$\begin{aligned}
I^{(0)}(X, |\xi|, t) &= -\frac{1}{2} \frac{ir}{\Lambda p^+} (X + \xi) \\
&\quad \times \sum_{i,j,k}^{4n+1} f_i f_j f_k \int \frac{d^2 \kappa_T}{(2\pi)^3} \\
&\quad \times \frac{\alpha_{ijk} F_2 + \alpha_{kji} F_1 + \eta_i^{3n} \eta_j^{4n} \eta_k^n}{d_{ij}^{(AB)} (-d_{ki}^{(AC)})} \quad (A29)
\end{aligned}$$

$$\begin{aligned}
I^{(0)}(X, -|\xi|, t) &= -\frac{1}{2} \frac{ir}{\Lambda p^+} (X - \xi) \\
&\quad \times \sum_{i,j,k}^{4n+1} f_i f_j f_k \int \frac{d^2 \kappa_T}{(2\pi)^3} \\
&\quad \times \frac{\alpha_{ijk} F_2 + \alpha_{kji} F_1 + \eta_i^{3n} \eta_j^{4n} \eta_k^n}{d_{ij}^{(AB)} d_{kj}^{(CB)}} \quad (A30)
\end{aligned}$$

$$\begin{aligned}
I^{(1)}(X, |\xi|, t) &= -\frac{ir}{\Lambda p^+} (X + \xi)^2 \sum_{i,j,k}^{4n+1} \alpha_{ijk} f_i f_j f_k \\
&\quad \times \int \frac{d^2 \kappa_T}{(2\pi)^3} \frac{-\kappa_T^2 \sin^2 \theta_T}{g_i^{(A)} d_{ij}^{(AB)} (-d_{ki}^{(AC)})} \quad (A31)
\end{aligned}$$

$$\begin{aligned}
I^{(1)}(X, -|\xi|, t) &= -\frac{ir}{\Lambda p^+} (X - \xi)^2 \sum_{i,j,k}^{4n+1} \alpha_{ijk} f_i f_j f_k \\
&\quad \times \int \frac{d^2 \kappa_T}{(2\pi)^3} \frac{-\kappa_T^2 \sin^2 \theta_T}{g_j^{(B)} d_{ij}^{(AB)} d_{kj}^{(CB)}} \quad (A32)
\end{aligned}$$

$$\begin{aligned}
I^{(2)}(X, |\xi|, t) &= -\frac{1}{2} \frac{ir}{\Lambda p^+} (X + \xi)^2 \sum_{i,j,k}^{4n+1} \beta_{ijk} f_i f_j f_k \\
&\quad \times \int \frac{d^2 \kappa_T}{(2\pi)^3} \frac{-\kappa_T^2 \sin^2 \theta_T}{h_i^{(A)} d_{ij}^{(AB)} (-d_{ki}^{(AC)})} \quad (A33)
\end{aligned}$$

$$\begin{aligned}
I^{(2)}(X, -|\xi|, t) &= -\frac{1}{2} \frac{ir}{\Lambda p^+} (X - \xi)^2 \sum_{i,j,k}^{4n+1} \beta_{ijk} f_i f_j f_k \\
&\quad \times \int \frac{d^2 \kappa_T}{(2\pi)^3} \frac{-\kappa_T^2 \sin^2 \theta_T}{h_i^{(A)} d_{ij}^{(AB)} d_{kj}^{(CB)}}. \quad (A34)
\end{aligned}$$

Integral $I^{(0)}$ can be calculated completely analytically, however we do not present the result here to make the paper more compact. It should be pointed out that the analytic formulas contain large sums of complicated complex expressions—therefore it is usually more efficient to perform all integrals numerically.

APPENDIX B: AXIAL TDA

In the axial channel we get

$$\begin{aligned}
A^{(i)}(X, \xi, t) &= -16iMN_c p^+ (Q_d \mathcal{J}^{(i)}(X, \xi, t) \\
&\quad - Q_u \mathcal{J}^{(i)}(-X, \xi, t)), \quad (B1)
\end{aligned}$$

where

$$\begin{aligned}
\mathcal{J}^{(0)}(X, \xi, t) &= \int \hat{d}k \frac{F_k F_{k+P_1}}{D_{k+P_1} D_{k+P_2} D_k} \{F_1 [M_{k+P_1} - M_{k+P_2} \\
&\quad - 2M_k] - F_2 (M_{k+P_2} - M_k) + M_k \\
&\quad + 2F_3 [M_{k+P_1} - M_k]\}, \quad (B2)
\end{aligned}$$

$$\begin{aligned}
\mathcal{J}^{(1)}(X, \xi, t) &= \int \hat{d}k \frac{F_k F_{k+P_1} (M_k - M_{k+P_2})}{k \cdot P_2 D_{k+P_1} D_{k+P_2} D_k} \\
&\quad \times \{F_1 [M_{k+P_1} M_k - M_{k+P_2} M_k - 2k^2 - 2k \cdot p] \\
&\quad + F_3 [M_{k+P_1} M_{k+P_2} - M_k M_{k+P_2} + M_k M_{k+P_1} \\
&\quad - k^2 + P_1 \cdot P_2]\}. \quad (B3)
\end{aligned}$$

Functions F_1, F_2 are the same as in the vector case while

$$F_3 = \frac{8\xi(\vec{k}_T \cdot \vec{q}_T)^2 + 2t\vec{k}_T \cdot \vec{q}_T(X-1)(2\xi^2 + \xi - 1) + t(\xi^2 - 1)(t(X-1)^2(1+\xi) - 4\xi k_T^2)}{2(1-\xi)(1+\xi)^2 t^2}. \quad (B4)$$

Calculations proceed quite similarly as before, although they are more involved. However, in the case of $\mathcal{J}^{(1)}$ additional difficulty arises if one wants to obtain a result for any n . Let us discuss this further.

The problematic part comes from the subterm of $\mathcal{J}^{(1)}$ containing more than 4 powers of $F(k)$. Using (A9) and (A10) this part reads

$$\mathcal{J}_A^{(1)}(X, \xi, t) = \frac{r^3}{\Lambda^2} \int \hat{d}k \frac{u_1^n u_2^{2n} (u_2^{2n} - u_1^{2n}) (F_1 + F_3)}{\kappa \cdot \bar{P}_2 G(u_1) G(u_2) G(u_3) u_3^n}. \quad (B5)$$

Notice that there is an additional u_3^n in the denominator which gives rise to multiple poles if $n \geq 2$. However if $n = 1$

$$\begin{aligned} \mathcal{J}_{A,n=1}^{(1)}(X, \xi, t) &= \frac{r^3}{\Lambda^2} \sum_{i,j}^5 \sum_k^6 f_i f_j \tilde{f}_k \int \hat{d}k \\ &\times \frac{(\eta_i \eta_j^4 - \eta_i^3 \eta_j^2)(F_1 + F_3)}{\kappa \cdot \bar{P}_2 (u_1 - \eta_i)(u_2 - \eta_j)(u_3 - \eta_k)}, \end{aligned} \quad (\text{B6})$$

where

$$\tilde{f}_i = \prod_{j=0, j \neq i}^5 \frac{1}{(\eta_i - \eta_j)} \quad (\text{B7})$$

and $\eta_0 = 0$, while η_1, \dots, η_5 remain solutions of $G = 0$. In order to avoid calculating residues of the multiple poles if $n \geq 2$, we choose to close the contour in such a way that multiple poles do not lie inside. The price we pay is that relevant expressions become more complicated. Moreover, although the pole coming from $\kappa \cdot \bar{P}_2$ does not give con-

tribution to $\mathcal{J}^{(1)}$, it does contribute to $\mathcal{J}_A^{(1)}$ and $\mathcal{J}_B^{(1)}$ separately where $\mathcal{J}^{(1)} = \mathcal{J}_A^{(1)} + \mathcal{J}_B^{(1)}$. This fact has to be taken into account when we decide to choose different contours for $\mathcal{J}_A^{(1)}$ and $\mathcal{J}_B^{(1)}$.

Now we are in a position to write the results. We use the same abbreviations as in the vector case, additionally we define

$$\begin{aligned} c_{ijk} &= -F_1(\beta_{ijk} + 2\eta_i^{3n} \eta_j^{4n} \eta_k^n) - 2F_3 \beta_{ijk} \\ &+ F_2 \alpha_{ijk} + \eta_i^{3n} \eta_j^{4n} \eta_k^n \end{aligned} \quad (\text{B8})$$

$$\begin{aligned} w_{ijk}^{(A,B,C)} &= F_1 r^2 \beta_{ijk} - F_1 \beta_{ijk} t^{(A,B,C)} + F_3 r^2 (\alpha_{ijk} + \beta_{ijk}) \\ &+ F_3 \beta_{ijk} s^{(A,B,C)}, \end{aligned} \quad (\text{B9})$$

where

$$t^{(A)} = \frac{-(1 + 2\xi)\kappa_T^2 + (1 + \eta_i - \vec{\kappa}_T \cdot \vec{q}_T)(2X - 1) + (X - 1)(X(2\xi - 1) + 1)\bar{p}^2}{X + \xi} \quad (\text{B10})$$

$$s^{(A)} = \frac{-(1 + \xi)\kappa_T^2 + (1 + \eta_i - \vec{\kappa}_T \cdot \vec{q}_T)(X - 1) - (X - 1)((X - 1)^2(1 - \xi) + 2(X + \xi))\bar{p}^2}{X + \xi} \quad (\text{B11})$$

$$t^{(B)} = \frac{(2\xi - 1)\kappa_T^2 + (1 + \eta_j + \vec{\kappa}_T \cdot \vec{q}_T)(2X - 1) - (X - 1)((2X - 1)(1 + \xi) + X - \xi)\bar{p}^2}{X - \xi} \quad (\text{B12})$$

$$s^{(B)} = \frac{(-1 + \xi)\kappa_T^2 + (1 + \eta_j + \vec{\kappa}_T \cdot \vec{q}_T)(X - 1) - (X - 1)((X - 1)^2(1 + \xi) + 2(X - \xi))\bar{p}^2}{X - \xi} \quad (\text{B13})$$

$$t^{(C)} = \frac{\kappa_T^2 + (1 + \eta_k)(2X - 1)}{X - 1} + (X - 1)\bar{p}^2 \quad (\text{B14})$$

$$s^{(C)} = 1 + \eta_k - 2\bar{p}^2. \quad (\text{B15})$$

We recall at this point that $\eta_0 = 0$, therefore although sums below run from unity, notation like “ d_{i0} ” makes sense.

(i) $|\xi| < X < 1$

$$\begin{aligned} \mathcal{J}^{(0)}(X, |\xi|, t) &= \mathcal{J}^{(0)}(X, -|\xi|, t) = \frac{ir}{\Lambda p^+} (X - 1) \\ &\times \sum_{i,j,k}^{4n+1} f_i f_j f_k \int \frac{d^2 \kappa_T}{(2\pi)^3} \frac{c_{ijk}}{d_{ki}^{(AC)} d_{kj}^{(CB)}} \end{aligned} \quad (\text{B16})$$

$$\begin{aligned} \mathcal{J}_A^{(1)}(X, |\xi|, t) &= \mathcal{J}_A^{(1)}(X, -|\xi|, t) \\ &= -\frac{ir^3}{\Lambda p^+} \sum_{i,j,k}^{4n+1} f_i f_j f_k (\eta_i^n \eta_j^{4n} - \eta_i^{3n} \eta_j^{2n}) \\ &\times \int \frac{d^2 \kappa_T}{(2\pi)^3} (F_1 + F_3) \\ &\times \left\{ \frac{(X + \xi)^{n+2}}{g_i^{(A)} d_{ij}^{(AB)} (-d_{ki}^{(AC)}) (-d_{0i}^{(AC)})^n} \right. \\ &+ \frac{(X - \xi)^{n+2}}{g_j^{(B)} d_{ij}^{(AB)} d_{kj}^{(CB)} (-d_{0j}^{(CB)})^n} \\ &\left. + \frac{(1 - \xi)^{n+2}}{(-g_i^{(A)}) g_j^{(B)} g_k^{(B)} (-g_0^{(B)})^n} \right\} \quad (\text{B17}) \end{aligned}$$

$$\begin{aligned}
\mathcal{J}_B^{(1)}(X, |\xi|, t) &= \mathcal{J}_B^{(1)}(X, -|\xi|, t) \\
&= \frac{ir}{\Lambda p^+} (X-1)^2 \sum_{i,j,k}^{4n+1} f_i f_j f_k \int \frac{d^2 \kappa_T}{(2\pi)^3} \\
&\quad \times \frac{w_{ijk}^{(C)}}{g_k^{(B)} d_{ki}^{(AC)} d_{kj}^{(CB)}}. \tag{B18}
\end{aligned}$$

(ii) $-|\xi| < X < |\xi|$

$$\begin{aligned}
\mathcal{J}^{(0)}(X, |\xi|, t) &= -\frac{ir}{\Lambda p^+} (X+\xi) \sum_{i,j,k}^{4n+1} f_i f_j f_k \\
&\quad \times \int \frac{d^2 \kappa_T}{(2\pi)^3} \frac{c_{ijk}}{d_{ki}^{(AC)} d_{kj}^{(CB)}} \tag{B19}
\end{aligned}$$

$$\begin{aligned}
\mathcal{J}^{(0)}(X, -|\xi|, t) &= -\frac{ir}{\Lambda p^+} (X-\xi) \sum_{i,j,k}^{4n+1} f_i f_j f_k \\
&\quad \times \int \frac{d^2 \kappa_T}{(2\pi)^3} \frac{c_{ijk}}{d_{ij}^{(AB)} d_{kj}^{(CB)}} \tag{B20}
\end{aligned}$$

$$\begin{aligned}
\mathcal{J}_A^{(1)}(X, |\xi|, t) &= -\frac{ir^3}{\Lambda p^+} \sum_{i,j,k}^{4n+1} f_i f_j f_k (\eta_i^n \eta_j^{4n} \\
&\quad - \eta_i^{3n} \eta_j^{2n}) \\
&\quad \times \int \frac{d^2 \kappa_T}{(2\pi)^3} \frac{(F_1 + F_3)(X+\xi)^{n+2}}{g_i^{(A)} d_{ij}^{(AB)} (-d_{ki}^{(AC)}) (-d_{0i}^{(AC)})^n} \tag{B21}
\end{aligned}$$

$$\begin{aligned}
\mathcal{J}_A^{(1)}(X, -|\xi|, t) &= -\frac{ir^3}{\Lambda p^+} \sum_{i,j,k}^{4n+1} f_i f_j f_k (\eta_i^n \eta_j^{4n} \\
&\quad - \eta_i^{3n} \eta_j^{2n}) \int \frac{d^2 \kappa_T}{(2\pi)^3} \\
&\quad \times \frac{(F_1 + F_3)(X-\xi)^{n+2}}{g_j^{(B)} (-d_{ij}^{(AB)}) (-d_{kj}^{(CB)}) (-d_{0j}^{(CB)})^n} \tag{B22}
\end{aligned}$$

$$\begin{aligned}
\mathcal{J}_B^{(1)}(X, |\xi|, t) &= -\frac{ir}{\Lambda p^+} (X+\xi)^2 \\
&\quad \times \sum_{i,j,k}^{4n+1} f_i f_j f_k \int \frac{d^2 \kappa_T}{(2\pi)^3} \\
&\quad \times \frac{w_{ijk}^{(A)}}{g_i^{(A)} d_{ij}^{(AB)} (-d_{ki}^{(AC)})} \tag{B23}
\end{aligned}$$

$$\begin{aligned}
\mathcal{J}_B^{(1)}(X, -|\xi|, t) &= -\frac{ir}{\Lambda p^+} (X+\xi)^2 \\
&\quad \times \sum_{i,j,k}^{4n+1} f_i f_j f_k \int \frac{d^2 \kappa_T}{(2\pi)^3} \\
&\quad \times \frac{w_{ijk}^{(B)}}{g_j^{(B)} (-d_{ij}^{(AB)}) (-d_{kj}^{(CB)})}. \tag{B24}
\end{aligned}$$

Notice, that some of the integrals are superficially divergent. Convergence is assured by the identity

$$\sum_{i=1}^{4n+1} f_i \eta_i^N = \begin{cases} 1 & \text{for } N = 4n; \\ 0 & \text{for } N < 4n; \end{cases} \tag{B25}$$

see [17] for the proof and discussion.

-
- [1] B. Pire and L. Szymanowski, Phys. Rev. D **71**, 111501 (2005).
[2] A. V. Belitsky and A. V. Radyushkin, Phys. Rep. **418**, 1 (2005).
[3] J. P. Lansberg, B. Pire, and L. Szymanowski, Phys. Rev. D **73**, 074014 (2006); *Exclusive Reactions at High Momentum Transfer* (World Scientific, Singapore, 2008); arXiv:0709.2567.
[4] B. C. Tiburzi, Phys. Rev. D **72**, 094001 (2005).
[5] A. Courtoy and S. Noguera, Phys. Rev. D **76**, 094026 (2007).
[6] W. Broniowski and E. R. Arriola, Phys. Lett. B **649**, 49 (2007).
[7] E. Ruiz Arriola and W. Broniowski, Phys. Rev. D **67**, 074021 (2003).
[8] P. Kotko and M. Praszalowicz, Acta Phys. Pol. B **40**, 123 (2009).
[9] D. Diakonov and V. Y. Petrov, Nucl. Phys. **B245**, 259 (1984); **B272**, 457 (1986).
[10] M. Praszalowicz and A. Rostworowski, Phys. Rev. D **64**, 074003 (2001).
[11] A. E. Dorokhov, Eur. Phys. J. C **42**, 309 (2005); Pis'ma Zh. Eksp. Teor. Fiz. **82**, 3 (2005) [JETP Lett. **82**, 1 (2005)].
[12] H. Pagels and S. Stokar, Phys. Rev. D **20**, 2947 (1979).
[13] J. S. Ball and T. W. Chiu, Phys. Rev. D **22**, 2542 (1980).
[14] B. Holdom, J. Terning, and K. Verbeek, Phys. Lett. B **232**, 351 (1989); **245**, 612 (1990).
[15] R. D. Bowler and M. C. Birse, Nucl. Phys. **A582**, 655 (1995); R. S. Plant and M. C. Birse, Nucl. Phys. **A628**, 607 (1998).
[16] M. R. Frank, K. L. Mitchell, C. D. Roberts, and P. C. Tandy, Phys. Lett. B **359**, 17 (1995).
[17] P. Kotko, M. Praszalowicz, Photon Distribution Amplitudes in Non-local Chiral Quark Model (unpublished).

- [18] A. Bzdak and M. Praszalowicz, *Acta Phys. Pol. B* **34**, 3401 (2003).
- [19] M. Praszalowicz and A. Rostworowski, *Phys. Rev. D* **66**, 054002 (2002).
- [20] M. Praszalowicz and A. Rostworowski, *Acta Phys. Pol. B* **34**, 2699 (2003).
- [21] V. Y. Petrov *et al.*, *Phys. Rev. D* **59**, 114018 (1999).
- [22] A. E. Dorokhov, W. Broniowski, and E. Ruiz Arriola, *Phys. Rev. D* **74**, 054023 (2006).
- [23] I. V. Anikin, A. E. Dorokhov, and L. Tomio, *Yad. Fiz.* **64**, 1405 (2001) [*Phys. At. Nucl.* **64**, 1329 (2001)].
- [24] A. E. Dorokhov, M. K. Volkov, and V. L. Yudichev, *Yad. Fiz.* **66**, 973 (2003) [*Phys. At. Nucl.* **66**, 941 (2003)].
- [25] A. E. Dorokhov, M. K. Volkov, V. L. Yudichev, report JINR-E4-2001-162, 2001.
- [26] A. E. Dorokhov and W. Broniowski, *Eur. Phys. J. C* **32**, 79 (2003).
- [27] S. i. Nam, H. C. Kim, A. Hosaka, and M. M. Musakhanov, *Phys. Rev. D* **74**, 014019 (2006); S. i. Nam and H. C. Kim, *Phys. Rev. D* **74**, 076005 (2006); **74**, 096007 (2006).
- [28] H. J. Behrend *et al.* (CELLO Collaboration), *Z. Phys. C* **49**, 401 (1991).
- [29] J. Gronberg *et al.* (CLEO collaboration), *Phys. Rev. D* **57**, 33 (1998).
- [30] B. Aubert *et al.* (The BABAR Collaboration), *Phys. Rev. D* **80**, 052002 (2009).
- [31] A. V. Radyushkin, arXiv:0906.0323.
- [32] M. V. Polyakov, arXiv:0906.0538.